Biological coordination chemistry of magnesium, sodium, and potassium ions. Protein and nucleotide binding sites

C. B. Black, H.-W. Huang and J. A. Cowan
Evans Laboratory of Chemistry, The Ohio State University, 120 West 18th Avenue, Columbus, OH 43210 (USA)

(Received 6 January 1993)

CONTENTS

Correspondence to: J.A. Cowan, Evans Laboratory of Chemistry, The Ohio State University, 120 West 18th Avenue, Columbus, OH 43210, USA.

0010-8545/94/$26.00
SSDI 0010-8545(93)00978-2

ABSTRACT

In this article, we review the structural chemistry of the alkali and alkaline earth metal cations (Mg^{2+}, Na^{+}, and K^{+}) with three classes of biological macromolecule (proteins, nucleic acids, and membrane lipids). Emphasis is placed on crystallographically well-characterized examples that illustrate the characteristic features of ligand type and coordination geometry that define the binding specificity and functional role (structural or catalytic) of these co-factors. Reflecting the availability of literature data, the focus of the review is directed toward magnesium chemistry. Four classes of magnesium coordination site (A–D) are defined according to whether the co-factor interacts predominantly with the protein or substrate, and serves either a structural or catalytic role. The distinction between inner and outer coordination modes is made. There is an apparent tendency for magnesium to bind to nucleic acids by extensive hydrogen bonding from waters of hydration to heteroatoms on bases and the ribose-phosphate backbone, while inner-sphere binding to proteins is promoted by the well-defined chelating pockets defined by protein residues. With regard to the functional role of the metal, the lability of these metal cofactors must be considered in the context of enzyme mechanism, inasmuch as the most stable structural configuration is not necessarily the competent coordination state for enzyme turnover. Oxygen ligation (from carboxylates, hydroxyl, water, or phosphate functionality) is common, although coordination by N-7 of guanosine is frequently observed in metal nucleotide structures in the solid state. In contrast to calcium-binding proteins, no general binding motifs have been clearly identified for magnesium sites in proteins.

ABBREVIATIONS

Ad	adenosine
ADP	adenosine diphosphate
ATP	adenosine triphosphate
DNA	deoxyribonucleic acid
ds	double-stranded
F1,6BP	fructose-1,6-bisphosphate
F1,6BPase	fructose-1,6-bisphosphatase
F2,6BP	fructose-2,6-bisphosphate
F6P	fructose-6-phosphate
GTP	guanosine triphosphate
dNMP	deoxynucleotide monophosphate
PEP	phosphoenolpyruvate
PFK	phosphofructokinase
2PG	2-phosphoglycerate
RNA	ribonucleic acid
Rubisco	ribulose-1,5-bisphosphate
RuBisCO	ribulose-1,5-bisphosphate carboxylase.

1. INTRODUCTION

There is increasing interest in the chemistry of the alkali and alkaline earth metals as structural and catalytic co-factors with proteins, enzymes, ribozymes, and

polynucleotides [1,2]. To this end, it is important to identify the characteristic features of ligand type and coordination geometry that define the binding specificity and functional role (structural or catalytic) of these co-factors. Previous crystallographic studies on calcium-binding proteins have demonstrated a number of common structural motifs that define the calcium site, for example, the EF-hand loop domains of regulatory proteins (such as calmodulin, troponin C, and calbindin), and the catalytic sites of hydrolytic enzymes (staphyloccocus nuclease, phospholipase A_2). In sharp contrast, the structural biochemistry of the remaining bulk mineral ions (Na^+, K^+, Mg^{2+}) is less well defined, although all are involved in the stabilization and/or activation of biological macromolecules. Only recently has a sufficiently large body of structural data been made available that allows some general comments to be made regarding magnesium binding sites on proteins and enzymes. Binding sites for K^+ and Na^+ remain for the most part poorly defined as a result of the lower affinity of proteins and nucleic acids for monovalent ions. In contrast, crystallographic definition of Mg^{2+} binding sites on oligonucleotides has been available for some time. In this review we will summarize what is known concerning the coordination environments of Mg^{2+}, K^+ and Na^+ for both proteins and nucleic acids, and attempt to identify the common structural principles that underlie the efficient binding of each. It will become evident that these are firmly grounded in the standard coordination chemistry established for each metal ion in solution and the solid state.

Magnesium tends to adopt octahedral coordination, with a marked preference for oxygen ligands (carboxylates, phosphates, hydroxyls, carbonyls, water). Sodium and potassium also adopt octahedral coordination, again showing a preference for oxygen donor ligands, although potassium can expand its coordination number to eight. Monovalent ions exhibit weak association to biological macromolecules and serve predominantly as bulk electrolytes that stabilize surface charge on proteins and nucleic acids. In contrast, divalent Mg^{2+} binds with higher affinity ($K_a \approx 10^2$–$10^5\ M^{-1}$), often serving a specific structural or catalytic role.

We will review the structural chemistry of these alkali and alkaline earth metal cations with three major classes of biological macromolecule (proteins, nucleic acids, and membrane lipids). Reflecting the availability of literature data, we will focus primarily on magnesium ion and emphasize crystallographically well-characterized examples. Little or no emphasis will be placed on the functional chemistry of the bound metal co-factor, while speculative analyses of low-resolution structural data will be avoided.

2. PROTEINS AND ENZYMES

2.1 Proteins that bind predominantly one magnesium ion per subunit

In this section we will review some representative, and structurally well-characterized magnesium (and to a far lesser extent potassium) coordination sites located

in enzyme and protein pockets. Each site is illustrated and described in the accompanying figures and legends, and a brief background to each enzyme is described in the text*. We will simply present some salient facts on protein binding domains and will leave the overview and analysis of underlying trends to the summary section at the end of the review.

2.1.1 Preliminary comments on magnesium binding to ATP and substrate molecules

Given the relatively high affinity of ATP^{4-} for Mg^{2+} ($K_a \approx 10^4\ M^{-1}$) and ADP^{3-} ($K_a \approx 10^3\ M^{-1}$), and the abundance of intracellular Mg^{2+} (~ 3 mM) [1,2], it is not surprising that the metal chelates are the most common physiological forms of these nucleotide substrates.

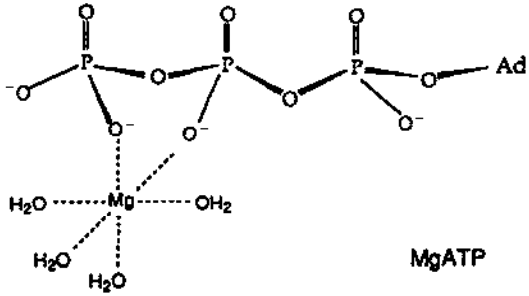

MgATP

Magnesium typically binds to the two terminal phosphates, either the β,γ-phosphates or α,β-phosphates, respectively, and promotes phosphoryl or nucleotidyl transfer reactions [2]. In most ATP-binding enzymes, the major contributor to the binding energy stems from hydrophobic interactions of the adenosine group with residues in an enzyme pocket, while the magnesium center interacts weakly, if at all, with protein side chains. Other proteins and enzymes that bind magnesium substrate complexes may also show minimal direct coordination between the metal site and protein residues. The affinity of the enzyme for Mg^{2+}(aq) is again weak in these cases, and so the protein does not provide an efficient binding domain for the divalent ion in the absence of substrate. In summary, Table 3 at the end of the review attempts clearly to delineate and classify proteins and enzymes that have intrinsic magnesium binding domains from those that bind the metal as a substrate complex.

2.1.2 Ha-ras p21

Ras genes are DNA sequences encoding MgGTP binding proteins (G-proteins) that are involved in mechanisms of cellular signal transduction. These constitute

* The figures usually show all protein contacts to the metal cofactor and also indicate the nature of the surrounding protein secondary structure in which a bound residue is found. Alpha helices and beta-sheets are indicated by the Greek symbols α or β, respectively, and specific structural elements designated by upper case letters or numerals. Intervening peptide domains linking secondary structure motifs are also indicated.

some of the few examples of magnesium-nucleotide-binding enzymes where protein sidechains play a significant role in the direct coordination of Mg^{2+}. Fig. 1(a) and (b) show the coordination environment of magnesium ion in Ha-ras p21 before and after transfer of the γ-phosphate of GTP. The structural changes that result from hydrolysis of MgGTP (the distance between Mg^{2+} and the hydroxyl of Thr35 doubles after phosphate transfer [3,4]), are important in regulating the function of the protein [5]. In this case, magnesium both activates the hydrolysis of GTP and stabilizes the resulting protein conformation.

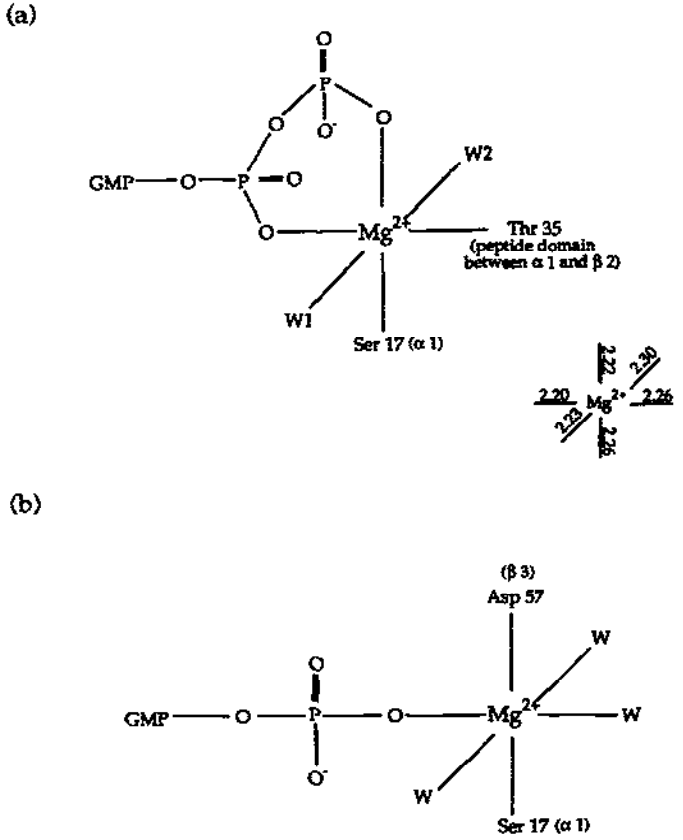

Fig. 1. (a) The 1.35 Å structure of the Ha-ras p21 GTP complex prior to hydrolysis. One of the bound waters provides a bridge to Asp 57, the residue which replaces the γ-phosphate. The secondary structure of the protein is indicated in the vicinity of the magnesium binding domain [5]. The inset shows bond distances in Å. Selected bond angles are noted in Table 4. (b) Ha-ras p21 after GTP hydrolysis. Asp 57 carboxylate takes up the position of the γ-phosphate. Thr 35 (shown here replaced by a water) is unlikely to bind to Mg^{2+} since the Mg^{2+}–(HO–Thr) spacing doubles to almost 4 Å after phosphate transfer [5]. It is possible that a water molecule bridges the threonine hydroxyl and magnesium, although there is no direct evidence for this.

2.1.3 Enolase

Enolase is a dimeric protein that catalyzes the interconversion of 2-phosphoglycerate and phosphoenolpyruvate. Each subunit requires magnesium for structural integrity and catalysis [6–8]. Enzyme activation follows a defined sequence of steps.

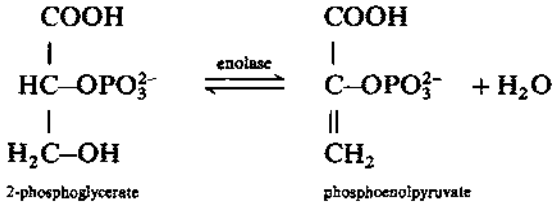

First, magnesium ion binds at the structural site; second, the resulting conformational change promotes substrate binding; and third, the substrate and enzyme pocket form an in situ binding site for the catalytic metal ion [4]. Figure 2 shows the high affinity conformational site with bound substrate (2-phosphoglycerate). The catalytic metal ion at the low affinity site was not co-crystallized with the protein.

2.1.4 Fructose-1,6-bisphosphatase

Fructose-1,6-bisphosphatase (F1,6BPase), a tetramer with two metal binding sites per 35 000 Da subunit [9,10], is an important enzyme in the glycolytic pathway (Scheme 1). It functions in tandem with phosphofructokinase, catalyzing the dephosphorylation of fructose-1,6-bisphosphate (the product of the phosphofructokinase reaction). Figure 3 shows the active site of fructose-1,6-bisphosphatase co-crystallized with the substrate analogue fructose-2,6-bisphosphate.

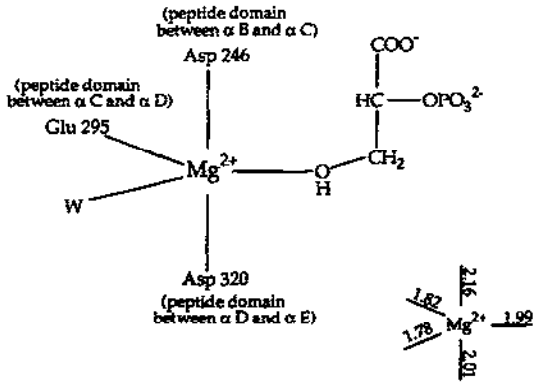

Fig. 2. The high affinity conformational site proposed for yeast enolase co-crystallized with 2-phosphoglycerate. The magnesium-bound water is believed to be strongly polarized and basic enough to abstract a proton from C-2 on the substrate [4]. Notice the unusual five-coordinate geometry of the magnesium ion and the surrounding secondary structure that is dominated by random strand sequences linking α-helices B, C, D and E. The inset shows bond distances in Å. Selected bond angles are noted in Table 4.

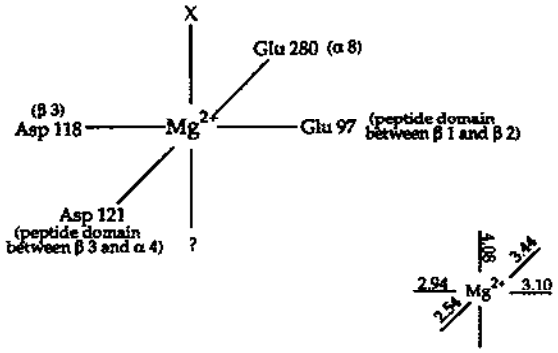

Fig. 3. The crystallographically defined magnesium binding site in fructose-1,6-bisphosphatase (isolated from pig kidney). X represents the 2-phosphate of a substrate analogue (fructose-2,6-bisphosphate) that was co-crystallized with the enzyme. The identity of the sixth ligand remains uncertain since no protein sidechains or water molecules were observed within 4 Å of the metal co-factor [9]. The secondary structure of the protein around the metal binding site is indicated [11]. The inset shows bond distances in Å. Selected bond angles are noted in Table 4.

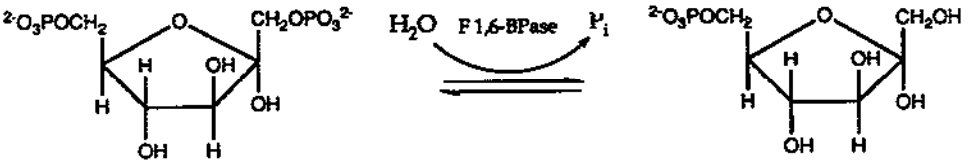

fructose 1,6-bisphosphate fructose 6-phosphate

Scheme 1.

2.1.5 Alkaline phosphatase

Alkaline phosphatase (so called because it exhibits maximal activity ca. pH 8) catalyzes hydrolysis of the terminal 5'-phosphate from DNA [12,13]. Each 47 kDa subunit of the homodimer requires two zinc ions and one magnesium for full catalytic activity [14]. The binuclear zinc center forms the catalytic site and hydrolysis proceeds by phosphorylation of a serine residue. Magnesium ion enhances the catalytic activity of the enzyme by 20% [15], although there is no evidence for direct participation in binding or catalysis [14]. Figure 4 shows how magnesium appears to serve a minor structural role [14,15], hydrogen bonding the substrate through the metal-bound water.

$$E + ROPO_3^{2-} \rightleftharpoons E.\ ROPO_3^{2-} \rightarrow E\text{-}PO_3^{2-} \xrightarrow[H_2O]{} E + HPO_4^{2-}$$
$$\downarrow ROH$$

2.1.6 Che Y

Bacterial chemotaxis is a motional response of bacteria to chemical substances. Four proteins are involved in the transfer of a signal from the transducer (receptor proteins in the membrane) to the flagellar motor by a pathway that involves protein

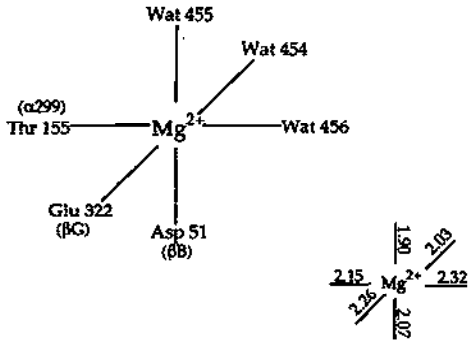

Fig. 4. The magnesium ion in the active site of *E. coli* alkaline phosphatase is bridged to the catalytic binuclear zinc site through Asp 51 [14]. In this case, magnesium cross-links several secondary structure motifs (2β sheets, 1α helix) [16]. The inset shows bond distances in Å. Selected bond angles are noted in Table 4.

phosphorylation. Che Y, which regulates the clockwise rotation of the flagella (proteinaceous tentacles that propel a bacterial cell at speeds of up to 50 $\mu m\ s^{-1}$), is activated by phosphorylation of Asp 57, while Asp 13 and Asp 12 appear to be of importance for catalysis [17]. On the basis of one highly ordered solvent molecule, Volz and Matsumura have proposed the structural model shown in Fig. 5 for the essential magnesium co-factor [18].

2.1.7 *Ribonuclease H*

E. coli ribonuclease H (RNase H) is a 17.5 kDa monomeric endonuclease that specifically cleaves the ribonucleotide strand of RNA.DNA hybrids. Magnesium ion

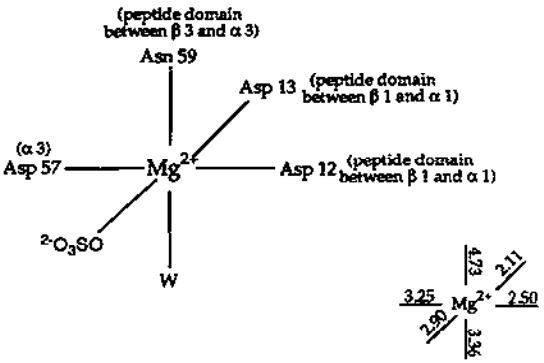

Fig. 5. The metal binding site of Che Y shows a bound sulfate that co-crystallized from solution. The active site magnesium was identified in the 1.7Å resolution electron density map through the presence of a highly ordered solvent molecule located in the most likely position for a magnesium ion. An additional metal-bound solvent water was not identified in the crystal structure but is likely to be present since the remaining ligands show a regular octahedral coordination geometry [18]. The inset shows bond distances in Å. Selected bond angles are noted in Table 4.

is an essential co-factor for enzyme activity with a proposed binding domain comprising two Asp and one Glu residue(s) [19]. There is a large degree of structural homology and identity of active site residues with the RNase H domain of retroviral reverse transcriptase [20–22].

2.2 *Proteins that bind multiple magnesium ions per subunit*

Many protein kinases, for example phosphoglycerate kinase [23], pyruvate kinase [24], adenylate kinase [25], and hexokinase [26,27] weakly bind a second Mg^{2+} in addition to MgATP. The function of this second metal ion is unclear but may contribute to the maintenance of structural integrity at the active site (e.g. phosphofructokinase), or possibly lower the activation barrier for group transfer (e.g. phosphoryl transfer by phosphoglycerate kinase). The most thoroughly characterized examples are described below.

2.2.1 *Xylose (glucose) isomerase*

Xylose (glucose) isomerase is a tetrameric enzyme made up of four identical 43 000 Da subunits. Two metal ions appear to bind per subunit with an inter-magnesium distance of less than 5 Å [28].

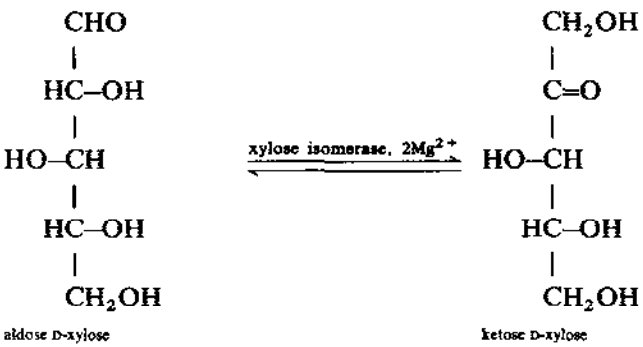

On the basis of crystallographic evidence, the coordination geometry at one site (metal 1) appears to switch from tetrahedral to octahedral after substrate binding (Fig. 6(a) and (b)), while the second site (metal 2) maintains the same inner coordination sphere whether or not substrate is present (Fig. 6(c) and (d)) [29]. This is consistent with the 1,2 hydride shift mechanism proposed previously [31]. As might be anticipated, there is some confusion as to whether the first site is actually tetrahedral (Fig. 6(b)), or possibly penta- or hexacoordinate. If the former, this will represent one of the few characterized examples of a tetrahedrally coordinated Mg^{2+} ion.

2.2.2 *Phosphofructokinase*

Phosphofructokinase is an $\alpha_2\beta_2$ tetramer that catalyzes the phosphorylation of fructose-6-phosphate to yield fructose-1,6-bisphosphate by phosphoryl transfer

(a)

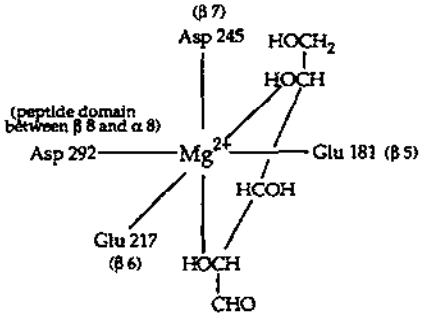
(β 7)
Asp 245
HOCH2
HOCH
(peptide domain between β 8 and α 8)
Asp 292
Mg2+
Glu 181 (β 5)
HCOH
Glu 217
(β 6)
HOCH
CHO

(b)

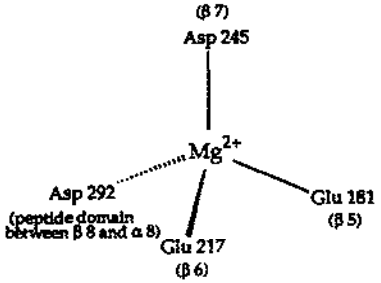
(β 7)
Asp 245
Mg2+
Asp 292
(peptide domain between β 8 and α 8)
Glu 181
(β 5)
Glu 217
(β 6)

(c)

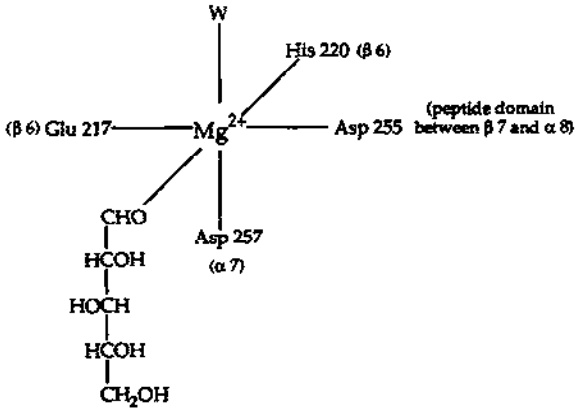
W
His 220 (β 6)
(β 6) Glu 217
Mg2+
Asp 255
(peptide domain between β 7 and α 8)
CHO
HCOH
HOCH
HCOH
CH2OH
Asp 257
(α 7)

(d)

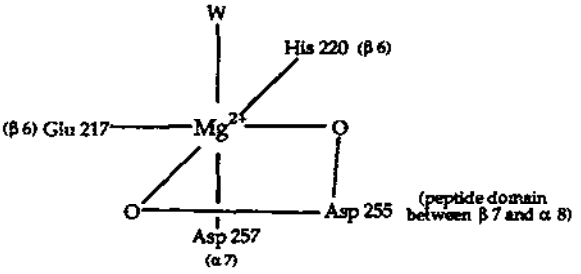
W
His 220 (β 6)
(β 6) Glu 217
Mg2+
O
O
Asp 255
(peptide domain between β 7 and α 8)
Asp 257
(α 7)

from MgATP. The enzyme contains both catalytic (β) and regulatory (α) subunits. Each 35 kDa subunit possesses three Mg^{2+} binding sites. The substrate binding site (fructose 6-phosphate) and the MgATP binding site are located in the catalytic domain. A third allosteric site binds either MgADP or phosphoenolpyruvate. Two

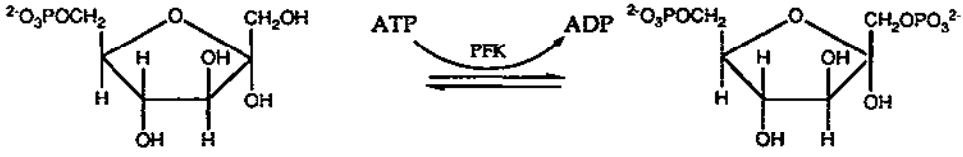

fructose 6-phosphate fructose 1,6-bisphosphate

magnesium ions have been identified with the catalytic domain (see Fig. 7(a)), while the third allosteric site is located at the interface of the α,β subunits (Fig. 7(b)) [32].

2.2.3 Pyruvate kinase

Pyruvate kinase catalyzes the conversion of phosphoenolpyruvate to pyruvate by transfer of phosphoryl to ADP. The reaction favors ATP formation and is essentially irreversible. The enzyme requires one monovalent cation (K^+) and two magnesium ions [one complexed to ADP/ATP (Fig. 8(b)), while the other is enzyme bound (Fig. 8(a))] [33,34].

phosphoenolpyruvate pyruvate

2.2.4 Ribulose-1,5-bisphosphate carboxylase

Ribulose-1,5-bisphosphate carboxylase (RuBisCO) is one of the most abundant enzymes in nature, constituting up to 50% of the soluble protein in leaves. This bifunctional protein catalyzes the initial steps of two distinct reaction pathways.

Fig. 6. (a) Metal site 1 of xylose isomerase from *Actinoplanes missouriensis* showing the bound substrate (aldose D-xylose). Glu 217 bridges the two Mg^{2+} ions that form the active site [see (c)] both with and without bound substrate (see (a)–(d)) [28,31]. The secondary structure of the surrounding protein matrix is predominantly β-sheet [30], cross-linked by Mg^{2+}. (b) Metal site 1 in the absence of substrate. No water molecules were located within 3 Å and the site appears tetrahedral [28,30,31]. This is one of the few examples of a protein-bound magnesium ion that adopts tetrahedral coordination. (c) Metal site 2 with bound substrate (aldose D-xylose). In contrast to site 1, this ion does not change geometry or ligands as a result of substrate binding [28,30,31]. (d) Metal site 2 in the absence of bound substrate. Residue Glu 217 bridges the metal sites (see (a)–(d)) while the carboxylate of Asp 255 chelates the metal in the absence of substrate [28,30,31].

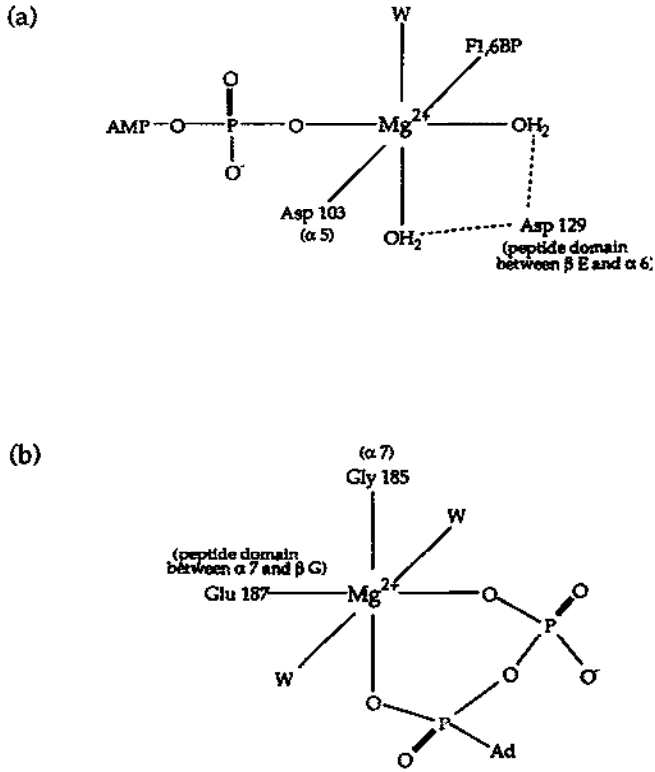

Fig. 7. (a) The closed form of the catalytic site of *E. coli* phosphofructokinase after product release. Asp 129 is hydrogen bonded to the waters of hydration [32]. (b) The effector site (site three) in *E. coli* phosphofructokinase with the allosteric activator, ADP. Note that Gly 185 is bound to the magnesium through the backbone carbonyl [32].

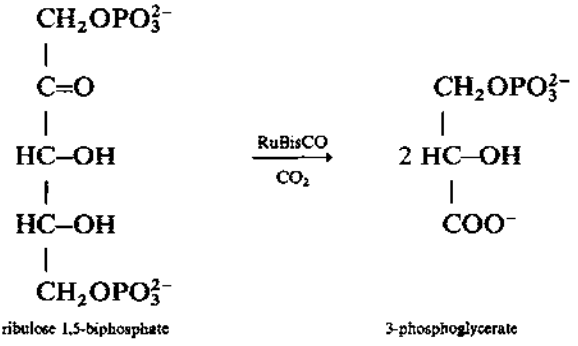

ribulose 1,5-biphosphate 3-phosphoglycerate

First, in the "dark" reactions of photosynthetic pathways the carboxylation of ribulose-1,5-bisphosphate yields two molecules of 3-phosphoglycerate. The magne-

(a)

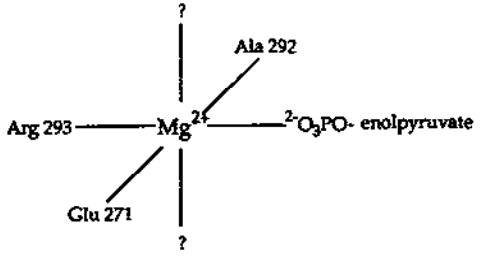

(b)

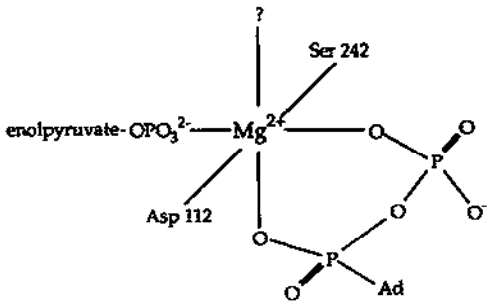

Fig. 8. (a) Part of the coordination environment for the enzyme-bound magnesium ion in the active site of pyruvate kinase, also showing bound substrate. Both Arg 293 and Ala 292 bind to the ion through backbone carbonyls. The precise coordination details of the cis/trans orientations of the ligands are uncertain [34,35]. The coordination sphere should be regarded as a good schematic illustration of the bound ligands. (b) The nucleotide binding site in skeletal muscle pyruvate kinase. This site is linked to the enzyme binding site (Fig. 8(a)) through the phosphoenolpyruvate molecule. Again, the precise details of the coordination geometry are uncertain [34].

sium ion stabilizes the intermediate carbamate following carboxylation of a lysine residue by CO_2. Secondly, the enzyme oxidizes ribulose-1,5-bisphosphate to give phosphoglycolate and 3-phosphoglycerate in photorespiration [36,37,39]. Figure 9(a) and (b) show the coordination environment of the ternary complex and the quarternary complex, respectively. Magnesium binds to the enzyme only after carbamate formation. Subsequently, substrate can favorably bind to this activated enzyme complex.

2.2.5 *Glutamine synthetase*

Glutamine synthetase is a complex enzyme comprising 12 identical 51 kDa subunits and six active sites [41–43]. Two metal ions, with an intersite spacing of

(a)

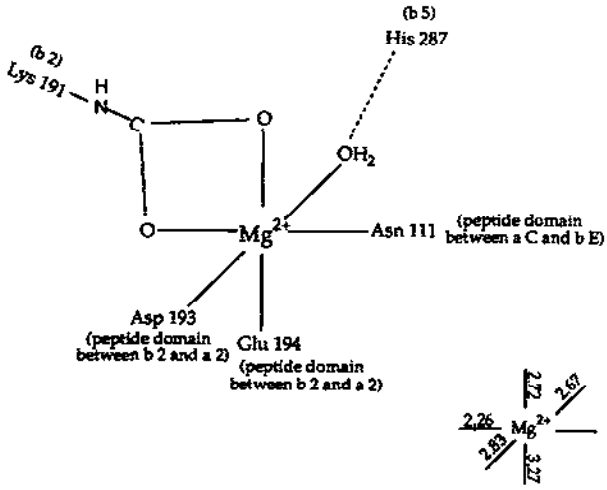

(b)

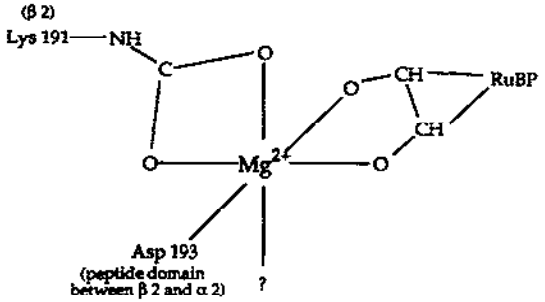

Fig. 9. (a) The active site of RuBisCO (from *R. rubrum*) showing the coordination sphere of magnesium ion prior to substrate binding to the activated enzyme. His 287 hydrogen bonds to metal-bound water. At the current limit of resolution it is not clear whether the nitrogen or oxygen on Asn 111 is bound to magnesium [38], although (a priori) one might expect oxygen ligation. Note also the predominance of β-sheet structure defining the metal binding site [40]. Rb = Rubisco. The inset shows bond distances in Å. Selected bond angles are noted in Table 4. (b) Active site coordination geometry after substrate (ribulose-1,5-bisphosphate) binding and carboxylation of Lys 191 to form the activated carbamate. The sixth site has not been clearly identified. Glu 194 moves to a distance greater than 2.7 Å from the magnesium ion, but may hydrogen bond to a bound water molecule [38,40].

5.8 Å (illustrated in Fig. 10(a) and (b)), are required for optimal activation of each subunit [41]. The enzyme is important for the regulation of cellular nitrogen metabolism, catalyzing the condensation of ammonia and glutamate to form glutamine. The crystallographic data shown in Fig. 10(a) and (b) were obtained on a Mn^{2+} derivative.

(a)

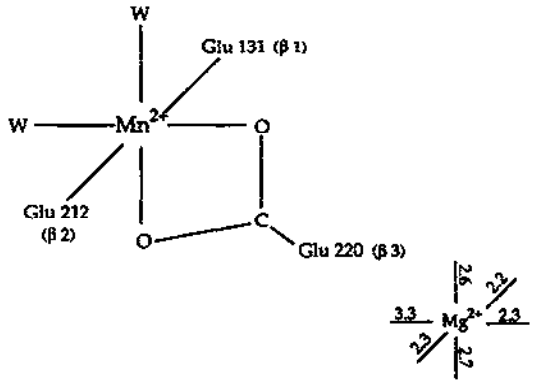

(b)

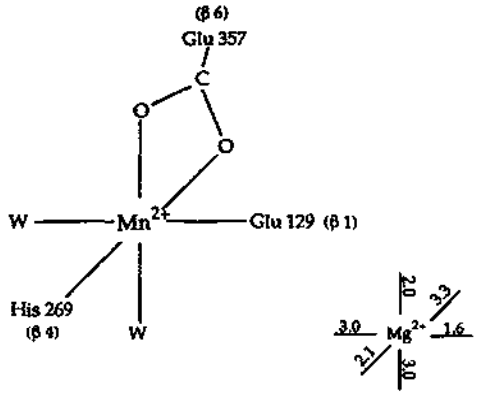

Fig. 10. (a) Structural details of the manganese derivative of glutamine synthetase (isolated from *S. typhimurium*) showing the inner enzyme-bound metal that forms part of the substrate binding site. One of the coordinated waters forms a bridge between the two metal sites (Fig. 10(b)). Glu 220 chelates as a bidentate ligand [44]. The inset shows bond distances in Å. (b) The outer magnesium binding site of glutamine synthetase (again identified as the manganese derivative). This site is the most likely location for MgATP, although the ATP ligand was not co-crystallized in this structure. A coordinated water molecule bridges the two metal ions. Either Glu 357 or Glu 129 serves as a bidentate ligand (Glu 357 is assumed for illustrative purposes) since in both cases the second carboxylate oxygen atoms lie 3.3 Å from the manganese ion. Note that a histidine nitrogen binds directly to the manganese ion [44]. It is not clear if His would bind to Mg^{2+} in this manner. The inset shows bond distances in Å.

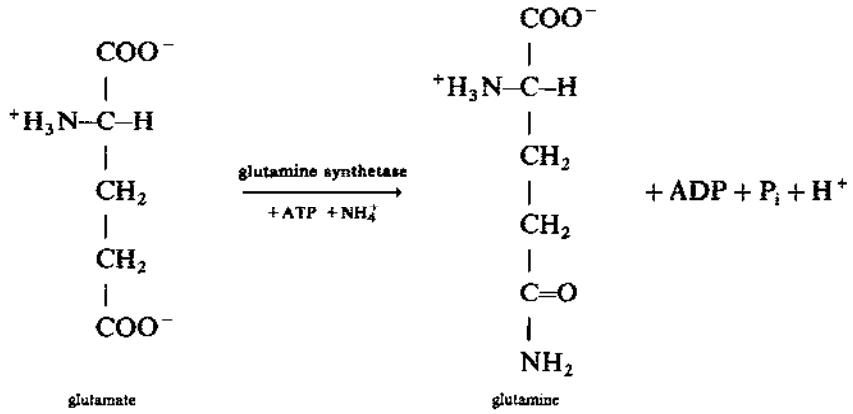

2.2.6 3′,5′-Exonuclease domain of DNA polymerase I

The 103 kDa Klenow fragment of DNA polymerase I contains both 5′,3′-polymerase and 3′,5′-exonuclease activities. These two domains function synchronously to provide error-free primed synthesis of DNA. The exonuclease site is located approximately 30 Å from the polymerase site [45]. The exonuclease domain binds at least two (Fig. 11), and possibly three divalent metal ions. Zinc is believed to bind at the higher affinity tetra- or pentacoordinate site (site A), while site B appears to be occupied either by a penta- or hexacoordinate magnesium ion [46]. The binding domain for the putative third metal ion is poorly defined.

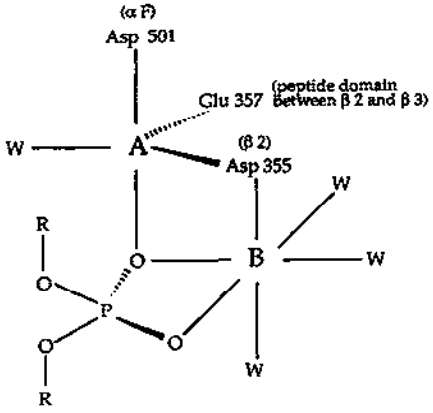

Fig. 11. The 3′-5′-exonuclease site in the Klenow fragment of *E. coli* DNA polymerase I [46]. Site B site (believed to be either penta- or hexacoordinate) is most likely a magnesium binding site. Site A (tetra- or pentacoordinate) maintains a high affinity for divalent zinc ions. Ion B is believed to activate the phosphodiester bond toward nucleophilic attack while promoting the departure of the 3′-oxygen. The carboxylate oxygens of Asp 355 bridge sites A and B [47]. The weakly bound magnesium (site B) was only identified in the presence of dNMP [46,48,49].

2.3 Potassium-activated enzymes

The importance of potassium ion for activation of enzymes was first recognized in the early 1940s during studies on pyruvate kinase. Since then, many enzymes have been shown to exhibit either a structural (e.g. β-galactosidase [50]) or catalytic dependence on K^+. In the case of pyruvate kinase, potassium appears to stabilize the enolate intermediate and may also aid in the alignment of the phoshoryl group for nucleophilic attack (Fig. 12) [51,52]. In comparison with Mg^{2+}, the lower charge density of K^+ results in low binding affinities to proteins and poor Lewis acidity. Consequently, K^+ typically serves as a biological electrolyte with few well-defined protein binding sites, but can also play a secondary role in catalysis and the maintenance of structural integrity.

3. METAL IONS AND MEMBRANES

Both alkali and alkaline earth metals stabilize biological membranes by charge neutralization after cross-linking the carboxylated and phosphorylated head groups of lipids. Metal ion binding raises the temperature of the phase transition and becomes more prominent with increasing charge on the cation [54]. In this context, metal ions also regulate endo- and exocytosis by influencing the fluidity and stability of membranes [55]. The bound cations also lower the permeability of the membrane toward water, aiding in the osmotic regulation of solvent transfer across the membrane [56], and inhibit chemical degradation. There is evidence for selective binding of Mg^{2+}, Ca^{2+}, Fe^{3+}, and Ni^{2+} at the membrane surface (Table 1). Surface binding of potentially toxic trace transition metal ions also forms part of a cells defence mechanism, while the influence of metal ions on membrane structure has important implications for the function of lipoproteins and ion channels.

4. METAL NUCLEOTIDE BINDING DOMAINS

Thus far we have not clearly distinguished the two principal binding modes for a metal ion with a biological molecule. These are indirect (outer sphere) associa-

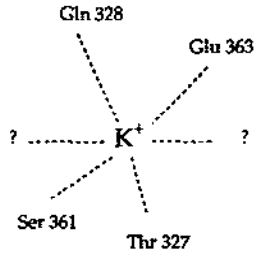

Fig. 12. A proposed binding site for the potassium ion in skeletal muscle pyruvate kinase. The identity of additional binding residues and the precise details of the coordination arrangement are unclear [34].

TABLE 1
Metal uptake by cell walls and membranes[a,b]

Organism	Component	Na^+	K^+	Mg^{2+}	Ca^{2+}	Mn^{2+}	Fe^{3+}
B. subtilis	Wall	2.70	1.94	8.22	0.40	0.80	3.58
B. licheniformis	Wall	0.91	0.56	0.40	0.59	0.66	0.76
E. coli-AB264	Peptidoglycan layer	0.290	0.060	0.035	0.038	0.052	0.010
E. coli-AB264	Outer membrane	0.081	0.025	0.019	0.020	0.012	0.233
E. coli-AB264	Cell envelope	0.042	0.082	2.56	0.035	0.140	0.200

[a]μmol metal (mg dry weight)$^{-1}$.
[b]See ref. 53.

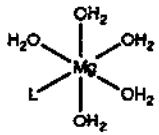

inner sphere

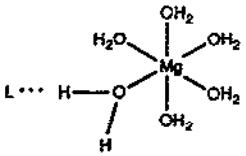

outer sphere

tion by hydrogen bond formation to solvent waters in the hydration sphere of the metal ion, and direct (inner sphere) coordination of a ligand to the metal center. Both modes of association have been identified in X-ray crystallographic studies of metal–oligonucleotide complexes. Outer sphere binding appears to be particularly common for interactions of magnesium ion, which adopts a regular octahedral hydration sphere with a Mg^{2+}–H_2O bond distance close to 2.0 Å, and oligonucleotides [57]. To distinguish clearly Mg^{2+} from the isostructural Na^+ ion, or to demonstrate direct coordination of a metal ion to a biological ligand, requires X-ray crystallographic data with a resolution of at least 1.5 Å. Beyond this limit, magnesium and sodium ions cannot be differentiated and each may be mistaken for solvent molecules.

As for proteins, most structural information on oligonucleotide complexes has been obtained for magnesium binding sites. Although the regular octahedral geometry is dominant, we shall see examples where magnesium forms ion clusters through bridging water molecules, and ligand loss resulting from steric restrictions. Usually, the favored sites for direct coordination to magnesium are phosphate oxygen and (surprisingly) N-7 of guanosine. Magnesium ion normally serves a structural role by stabilizing the sugar–phosphate backbone of oligonucleotides; however, a catalytic role is also likely for the reactions of ribozymes. In this section, we will review some characteristics of Mg^{2+} and Na^+ binding sites on oligonucleotides. Most of the available information has been deduced from a relatively small number of high-resolution structures.

4.1 Magnesium–DNA complexes

4.1.1 Outer sphere coordination

An octahedral hexahydrated magnesium ion has been identified on the Z-DNA obtained from a d(CGCGTG) sequence [58]. Three waters of hydration form hydrogen bonds with the wobble base pair G8T5. Two other water molecules were found to hydrogen bond to the sugar phosphate backbone of an adjacent base residue. Figure 13 shows the structural detail of the magnesium complex associated with the base pair GT, while Fig. 14 illustrates the corresponding magnesium binding site at the base pair G8C5 of the complementary Z-DNA oligomer d(CGCGCG) [59]. In the latter case, the aquated magnesium ion moved somewhat closer to the purine residue and only two Mg^{2+}-bound water molecules were able to hydrogen bond to the G8C5 base pair. The $Mg(H_2O)_6^{2+}$ ion forms an additional H-bond to the O-6 atom of G4 in the neighboring base pair G4C9. A symmetry-related hydrated magnesium ion was also noted in the same DNA complex [59], which forms a single H-bond to the oxygen of P10. The DNA oligomer d(CGCGFG), where F represents a fluorinated uridine, provides a related example with a $Mg(H_2O)_6^{2+}$ binding site located at a similar position to those found with d(CGCGTG) and d(CGCGCG), although the H-bond patterns from the complexed waters and the corresponding wobble base pair (F5G8) are different [60]. For example, Fig. 15 shows that one

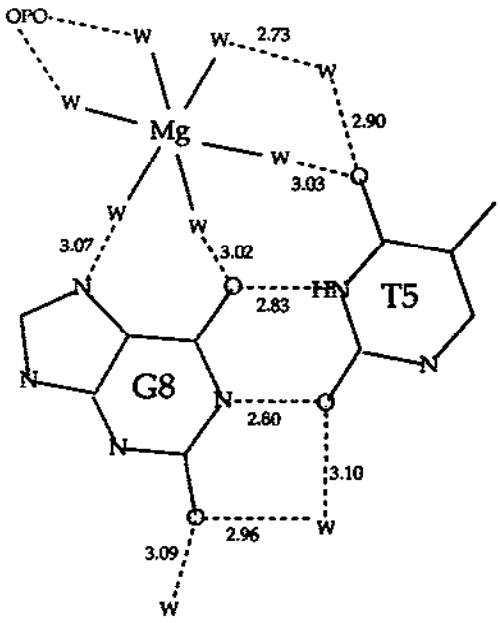

Fig. 13. Schematic diagram of the magnesium ion complex with the wobble base pair GT in d(CGCGTG). Hydrogen bonds are indicated by broken lines and the distances (in Å) are defined by the oxygen–oxygen internuclear spacing. Water molecules are represented by W and the backbone phosphate by OPO.

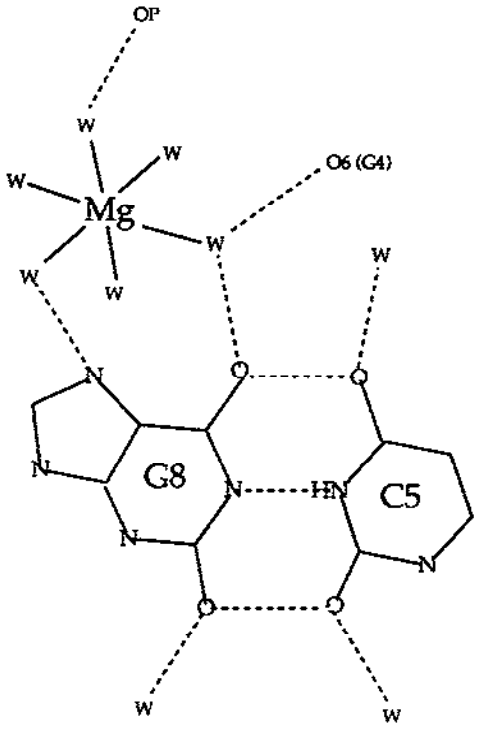

Fig. 14. Magnesium ion complex with a GC base pair in d(CGCGCG). Phosphate oxygens are indicated by PO. The residue name and number are indicated in parentheses.

water molecule forms two H-bonds to O-4 of 5-FU and O-6 of G8, respectively, while a second water molecule forms two H-bonds to O-6 and N-7 on the same base G8. It has been suggested that the observed differences for complexation of $Mg(H_2O)_6^{2+}$ to the d(CGCGFG) and d(CGCGTG) oligonucleotides may be related to the distinct solvent organization in the vicinity of the fluorine atom of 5-fluorouridine versus the methyl group of thymidine [3].

Recently, a detailed study of the magnesium binding sites on the Z-DNA duplex obtained from d(CGCGCG) has been reported [61]. Five distinct binding environments for $Mg(H_2O)_6^{2+}$ (labeled as A, A′, B, B′ and B″) were identified (Fig. 16). At site A, the hydrated magnesium ion forms four H-bonds to three successive phosphates (P8, P9 and P10) along one strand of DNA. The symmetry-related complex at site A′ is also H-bonded to the phosphate oxygen of P5 and the ribose O-4′ of G6. Magnesium ion at site B is located at the entrance of the minor groove and bridges the two strands of the phosphate backbone. Three coordinated water molecules from the ion at site B are H-bonded to phosphate oxygens (P6 and P10). Site B′ is located on the convex surface of the Z-DNA major groove. The hydrated magnesium ion forms H-bonds to two G residues from complementary strands; O-6

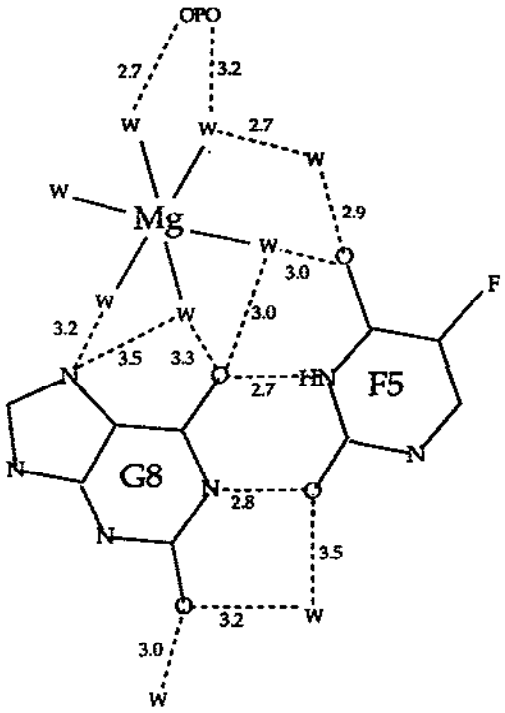

Fig. 15. Magnesium ion complex with the wobble base pair FG in d(CGCGFG). Hydrogen bonds are indicated by broken lines and the distances (in Å) are defined by the oxygen–oxygen internuclear spacing.

of G4 and N-7 of G8. The metal center at site B″ is rather distant from the DNA and only one H-bond is directed toward a phosphate group (P5). Figure 16 summarizes the coordination environment for each of these bound ions and shows the radial projection of the magnesium binding sites on the Z-DNA from the d(CGCGCG) nucleotide sequence. Although several of these sites may be unique to the crystal form, it has been suggested that the magnesium complexes A and B might also exist in solution. In addition to these $Mg(H_2O)_6^{2+}$ sites, five clusters of multiple magnesium centers were also identified in this DNA oligomer. These will be discussed in Sect. 4.1.3.

In a crystal lattice, magnesium ions are found to form not only intramolecular complexes with DNA oligomers, but may also form intermolecular links to neighboring molecules. For example, the crystal structure of the B-DNA sequence d(CGATTAATCG) shows a magnesium ion that links two helices [62]. Figure 17 shows two magnesium-bound water molecules that form hydrogen bonds to N-3 of A17 and O-2 of T5 in one helix, while two additional water molecules hydrogen bond to the phosphate oxygens of A3 in an adjacent DNA molecule. This kind of intermolecular interaction has also been noted in the crystal structure of a chiral phosphorothioate (R-form) analogue of B-DNA R-d[G(S)CG(S)CG(S)C] [63].

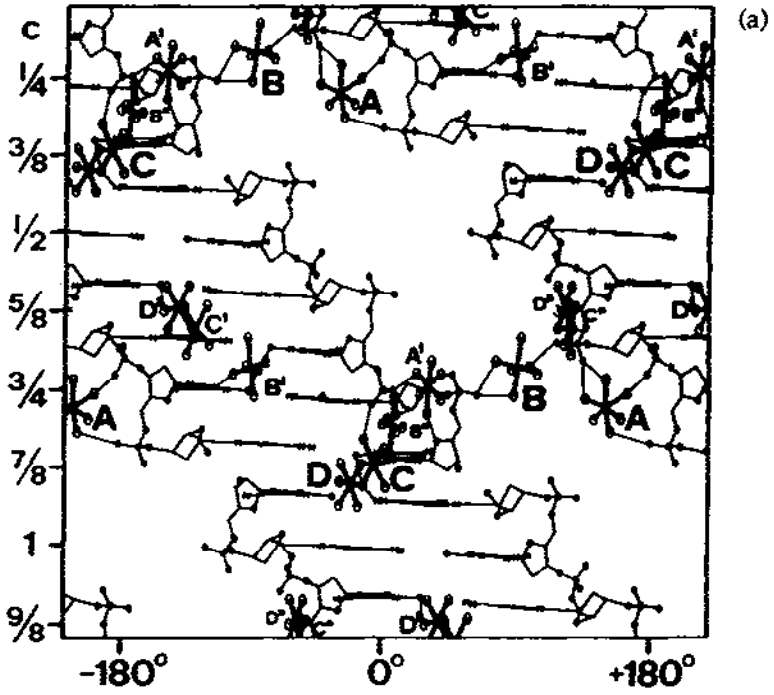

Fig. 16. (a) Radial projection of the magnesium ion complexes in d(CGCGCG). Hydrogen bonds between the ion complex and oligonucleotide are indicated by a thin solid line, while coordination between the ligands and the magnesium ion is indicated by heavy bars [adapted from ref. 61].

4.1.2 Inner sphere coordination

The examples above illustrate outer sphere binding of magnesium ion to oligonucleotides by formation of a hydrogen-bond network from coordinated water molecules. However, direct inner-sphere binding has also been observed in X-ray crystallographic data. For example, the structure of the methylated hexamer d(m^5CGTAm^5CG) shows one magnesium ion octahedrally coordinated to five water molecules and one phosphate oxygen of G2 [64]. It retains a regular octahedral geometry with Mg-OH_2 and Mg-phosphate distances of 2.0 Å. Figure 18 shows that two of the associated water molecules also form hydrogen bonds to neighboring backbone phosphates.

4.1.3 Magnesium clusters

Figure 18 shows two symmetry-related cation clusters that have been identified in the crystal structure of d(m^5CGTAm^5CG) [64]. Each cluster contains four cations, either magnesium or sodium, coordinated by water molecules in a slightly distorted octahedral environment. Magnesium ion typically adopts a regular octahedral geom-

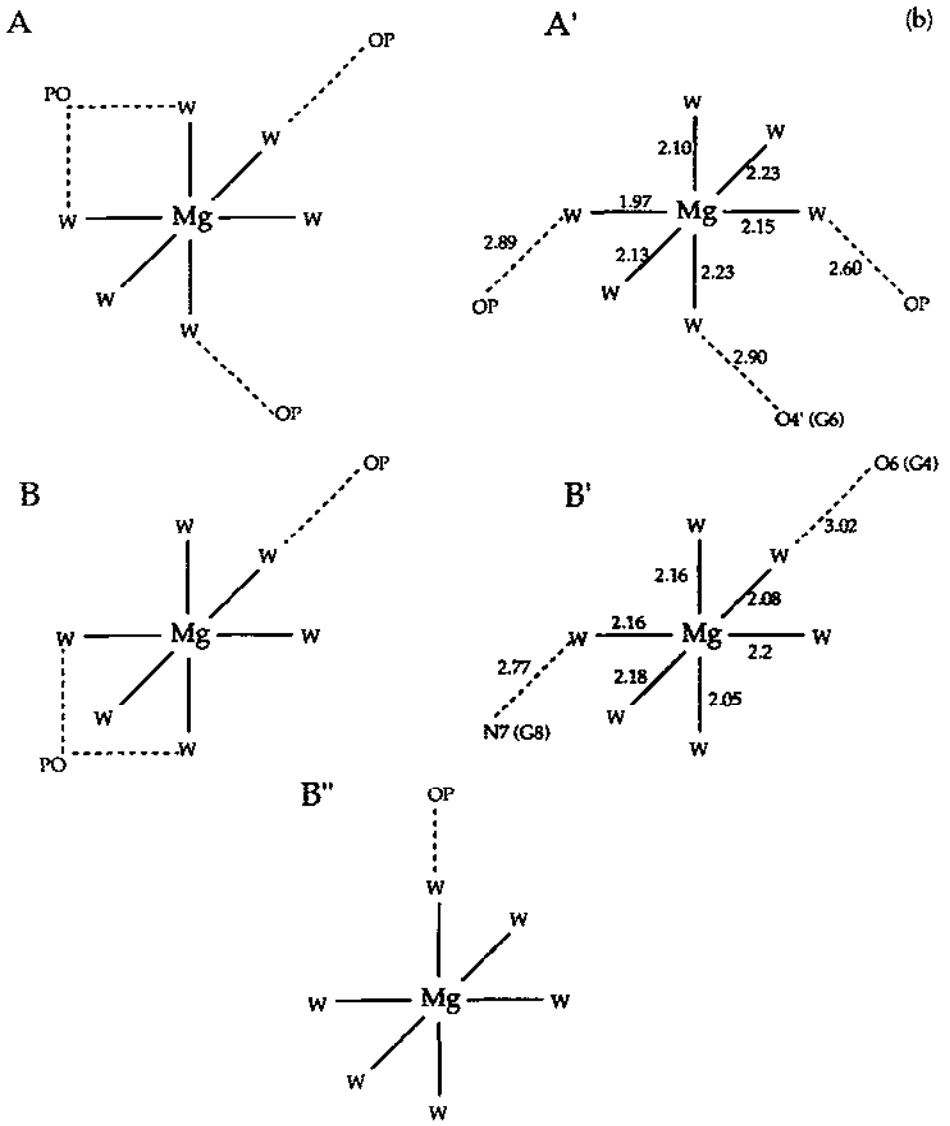

Fig. 16 (b) The coordination environment of each magnesium ion is illustrated for clarity. In this case, H-bonds are represented by broken lines, while distances (in Å) are defined by the oxygen–oxygen internuclear spacing. Bond distances are measured from the protein data bank. Selected bond angles are listed in Table 5.

etry with a magnesium-oxygen distance of 2 Å, while sodium ion often shows distortions from regular octahedral symmetry and variable sodium–oxygen distances ranging from 2.3 to 2.7 Å. On this basis, it has been suggested that two of the cations in the clusters A and A′ are likely to be Mg^{2+} (indicated in Fig. 18(b)). Mg^{2+} in

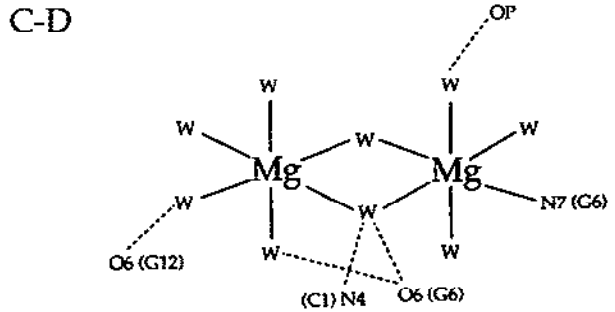

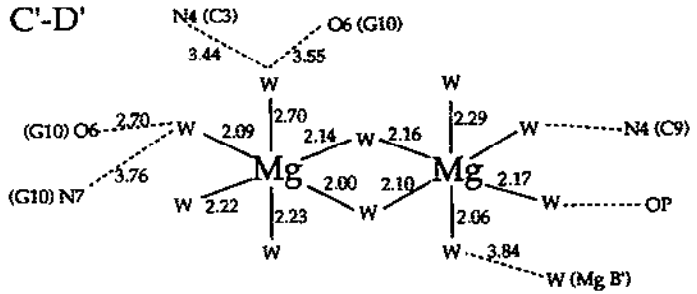

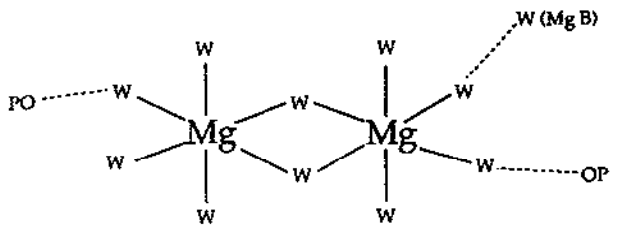

(b) (continued).

cluster A on the convex side of the major groove binds to N-7 of guanine, while the other ion (in cluster A') is directly coordinated to phosphate oxygen. The two outer octahedrally coordinated ions share edges with the two central octahedra, which themselves share a common face. The cluster on the convex side forms four H-bonds to nucleotide bases, while the ion cluster on the groove side forms H-bonds only to the phosphate backbone. It is interesting to note that the four-cation cluster may

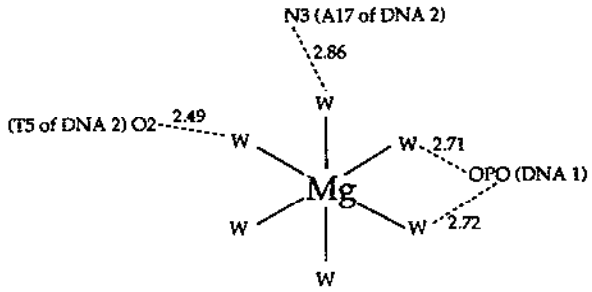

Fig. 17. Cross-linking of two DNA helices d(CGATTAATCG) by magnesium ion. Hydrogen bonds are indicated by broken lines and the distances (in Å) are defined by the oxygen–oxygen internuclear spacing.

serve as a "pseudospermine", which neutralizes the negatively charged phosphate backbone. Just as the spermine ligand has four charged centers separated by methylene (–CH_2–) groups, so the ion cluster contains four positively charged metals with the coordinated water molecules acting as spacer units.

Ion clusters have also been identified in the crystal structure of Z-DNA d(CGCGCG) (Fig. 16(b)) [61]. A dimeric magnesium complex (sites C and D), bridged by two water molecules, is located at the junction between two DNA hexamers. Mg^{2+} (C) binds to five water molecules and N-7 of G6. One of the shared water ligands forms two H-bonds; one to O-6 of G6 in the hexamer directly coordinated by Mg^{2+}(C), and the other to N-4 of C1 in the adjacent oligonucleotide. Besides this

(a)

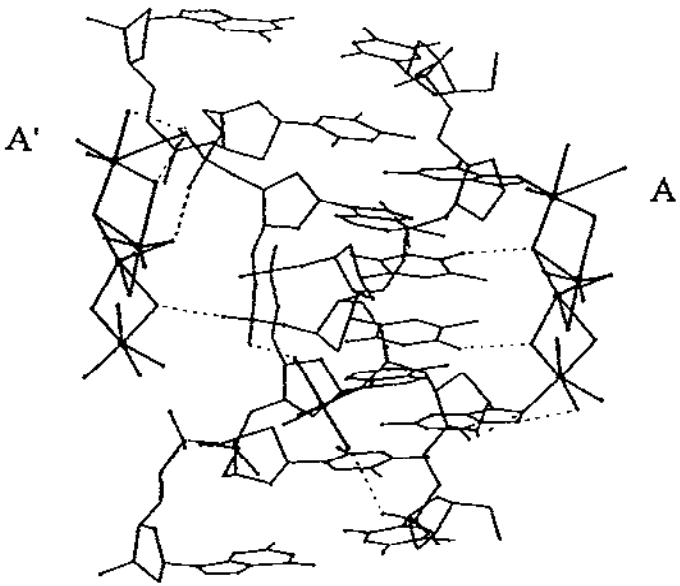

(b)

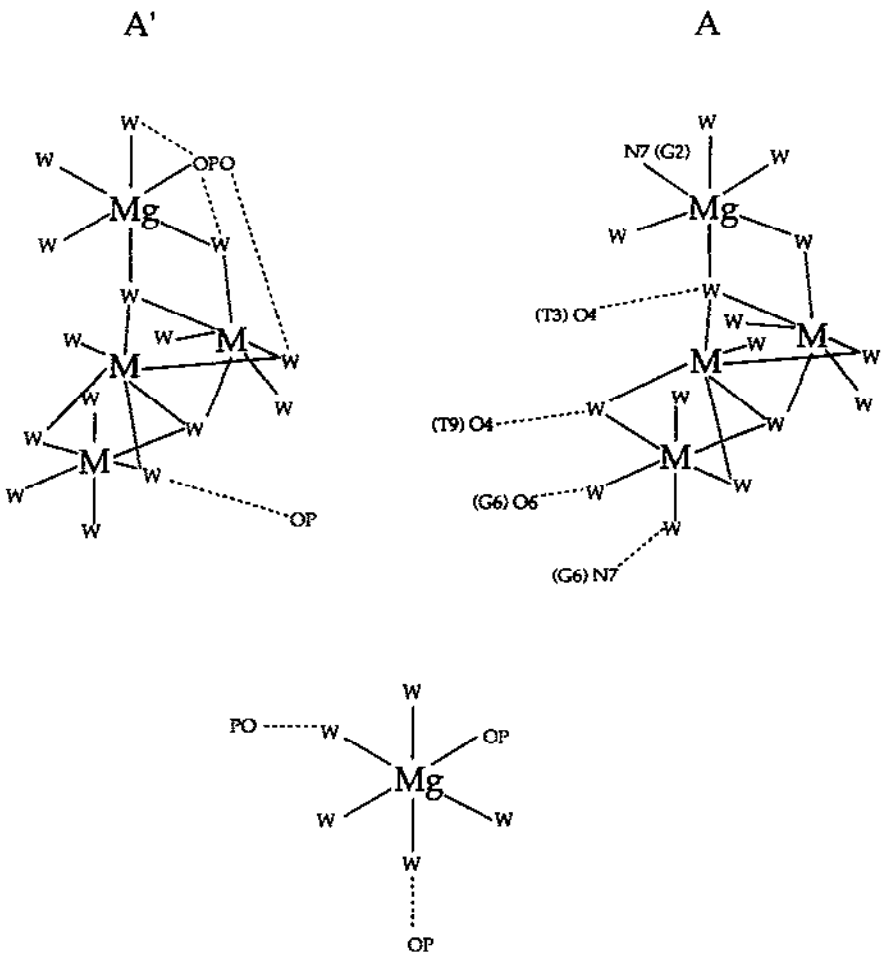

Fig. 18. (a) Skeletal diagram of the magnesium ion complexes with Z-DNA d(m^{5}CGTAm^{5}CG) [adapted from ref. 64]. (b) The coordination environments of the individual magnesium ions and ion clusters (A and A') are shown.

end-to-end intermolecular linkage, ion C also stabilizes the Z_{II} conformation of the phosphate backbone (P5)*. This Z_{II} conformation is further stabilized by a bridging water molecule that is linked to the magnesium ion complex B″ through the second hydration shell. It has been proposed that the magnesium ion at site C also exists in solution. In addition to the shared water molecule between ions C and D, two additional water molecules (coordinated to ion D) contribute to the stabilization of

* The Z_{II} conformation is a slight variation of the regular Z-conformation that arises in d(GpC) sequences when hydrated magnesium binds to the phosphate backbone. See ref. 78 for further details.

these contiguous oligonucleotides. One water ligand hydrogen bonds to O-6 of the Mg^{2+}(C)-coordinated G6, and the other forms an H-bond to O-6 of G12 in the adjacent oligonucleotide. A symmetry-related dimeric ion cluster C′–D′ has been located at a different surface site on the ds DNA molecule. This cluster complex interacts with the DNA by hydrogen bond formation from magnesium-bound water to (a) O-6 and N-7 of G10, (b) N-4 of C3, (c) the phosphate group of P9, and (d) ion B′. The third dimeric magnesium ion cluster identified in this structure is denoted C″–D″. This forms hydrogen bonds to the phosphate groups (P11 and P10) and also interacts with ion complex B.

4.1.4 Alternative coordination geometries for magnesium and sodium

In addition to regular octahedral coordination, magnesium ion has been found to adopt irregular geometries. A tetrahydrate magnesium ion $Mg(H_2O)_4^{2+}$ was located in the structure of Z-DNA d(CGCGCG) in the presence of magnesium and cobalt hexaammine [59]. This ion also coordinates directly to N7 of G6 and locks the local phosphate backbone into a Z_{II} conformation. It has been suggested that the loss of a water molecule from the octahedral complex results from the steric presence of a neighboring cobalt hexaammine.

With regard to sodium ion, an irregular complex was located in the major groove of d(5BrC-G-5BrC-G-5BrC-G) [65]. Figure 19 shows coordination to seven ligands (five water molecules, N-7 of G2, and the phosphate oxygen of C11); however, the coordination geometry of the sodium ion may be viewed as a distorted octahedron if the distant and weakly bound water ligand is excluded.

An interesting example of the role of bound potassium ion in polynucleotide chemistry comes from telomeric DNA. Telomeres are chromosomal DNA with a 3′-overhang of two repeating sequences that can form antiparallel guanine quadruplexes [66]. A cavity is created within the hairpin dimer by the O-6 oxygens of two stacked guanine tetrads. Fiber diffraction data and model building led to the proposal that this cavity is suitable for coordination of potassium ion in a cubic geometry, reflecting the ability of potassium, unlike the smaller sodium ion, to expand its coordination shell. Figure 20 shows the proposed structure of telomeric hairpin dimers and the coordination environment of potassium ion within the chelation cage.

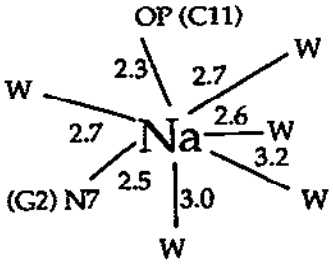

Fig. 19. Interaction of sodium ion and d(5BrC-G-5BrC-G-5BrC-G). Bond distances are noted in Å.

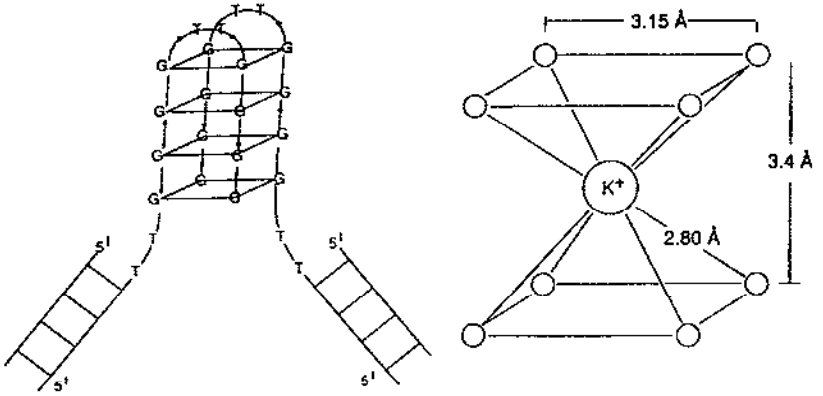

Fig. 20. Proposed structure of telomeric hairpin dimers and the coordination environment of potassium ion within the cage (adapated from ref. 66).

4.2 Magnesium binding sites on transfer RNA

Phenylalanine transfer RNA is one of the most thoroughly investigated RNA molecules. Crystallographic data have clearly identified at least four high-affinity magnesium binding sites [67–70] and a large number of ions are known to bind weakly ($K_a \sim 10^2\ M^{-1}$), although the structural details of the latter sites remain poorly characterized [71,72]. Figure 21 shows the locations of the four crystallographically characterized sites in yeast $tRNA^{Phe}$, all of which are placed in non-helical environments. A regular octahedral $Mg(H_2O)_6^{2+}$ is located at the turn formed by

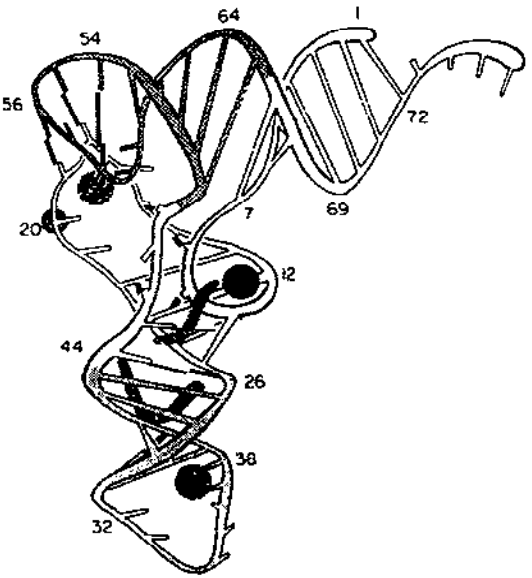

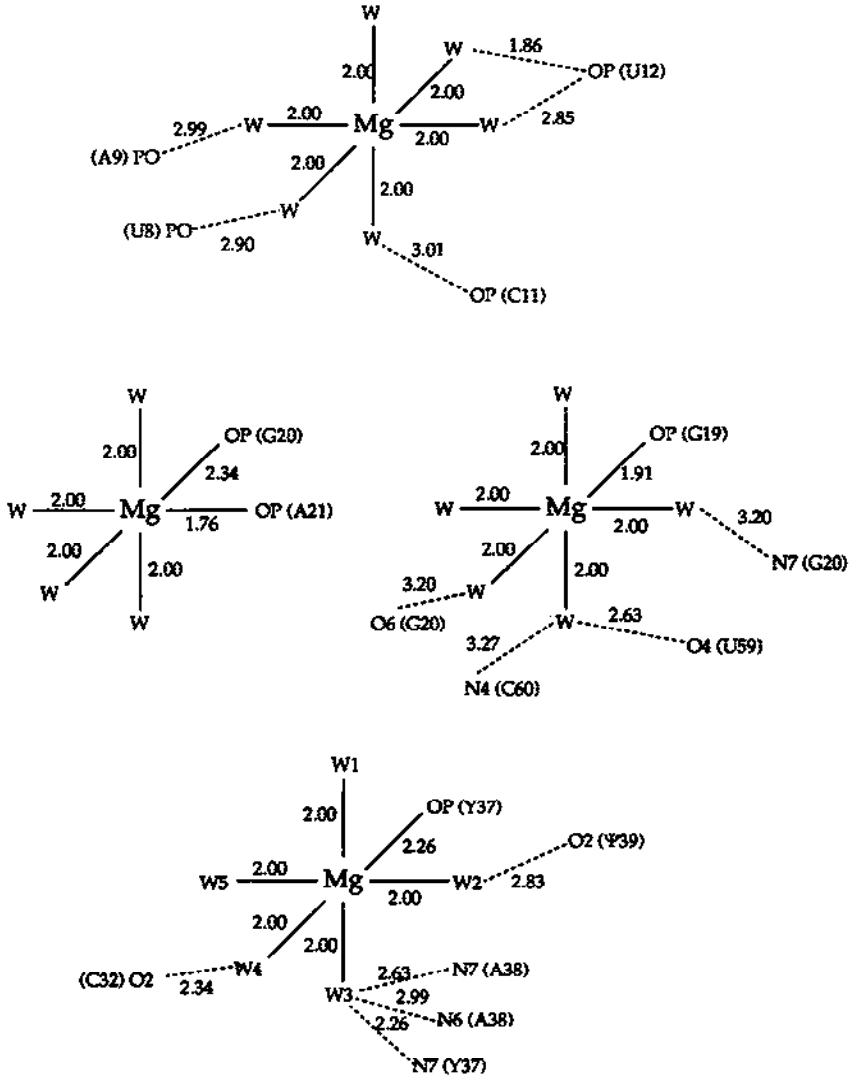

Fig. 21. Structurally characterized magnesium binding sites in $tRNA^{Phe}$ (adapted from ref. 70). Bond distances were obtained from the protein data bank. Hydrogen bonds are indicated by broken lines and the distances (in Å) are defined by the oxygen–oxygen internuclear spacing. Selected bond angles are listed in Table 5.

residues U8 to U12. This hydrated complex forms hydrogen bonds to the phosphate oxygens of U8, A9, C11 and U12. A second magnesium ion is located at the D loop and coordinates directly to the phosphate oxygen of G19. It also binds through an array of hydrogen bonds from the waters of hydration to the base heteroatoms of G20, U59 and C60. The third magnesium ion is also located in loop D and is coordinated by the phosphate oxygens of G20 and A21, and four water molecules

that are solvent exposed rather than forming H-bonds to any specific heteroatom of the tRNA molecule. A fourth magnesium ion complexes to tRNA at the anticodon loop. It binds directly to the phosphate oxygen of Y37 and directs H-bonds from the waters of hydration to the base heteroatoms C32, Y37, A38 and Ψ39.

Approximately 40–60 weaker magnesium binding sites have been determined for yeast $tRNA^{Phe}$ by ^{25}Mg NMR, crystallography, and equilibrium dialysis [71,72]. NMR studies suggest the ligand environment of these ions to be highly symmetric, and consistent with outer sphere binding.

4.3 Magnesium binding sites on ribozymes

Ribozymes catalyze site-specific RNA cleavage and splicing reactions. Group I introns, ribonuclease P, and hammerhead ribozymes each require divalent metal co-factors (especially Mg^{2+} or Mn^{2+}) for full catalytic activity [73–75]. Although two classes of metal binding site have been postulated for ribozyme activity (ions that serve a structural role and those involved in catalytic activation) [76], the details of the reaction mechanism and the role of the essential metal cations are not yet clear. There are many speculative structural models for the role of divalent metal ions in ribozyme chemistry, however, there is currently no crystallographic evidence to substantiate these ideas and so we will not comment further on this area.

5. SUMMARY

Few generalizations can yet be made concerning the coordination domains of magnesium, potassium, and sodium ions on biological macromolecules. Current literature reflects the wide variety of magnesium coordination sites in contrast to the more elusive binding sites of potassium and sodium. A few general points can, however, be made in view of the data summarized in this review.

Potassium and sodium typically serve as bulk electrolytes in biological systems to maintain electrochemical gradients and provide charge neutralization. Pyruvate kinase is one of the few examples where a single potassium ion is known to serve a specific structural role by bridging the enzyme and substrate pyruvate, and possibly aligning the substrate in the active site [51]. In general, however, both Na^+ and K^+ tend to form weak complexes to proteins, enzymes, lipid membranes and nucleic acids. In contrast, specific structural and catalytic roles have been identified for magnesium ion in the regulation of protein structure, enzyme catalysis, membrane stabilization, ion transport, and cell growth.

Table 2 summarizes the relevant details of the coordination environments for the protein binding sites described in Sect. 2. From this data we have identified several categories of binding site for magnesium-dependent enzymes (Table 3) according to the functional role of the cofactor. Type A sites are characterized by close association of magnesium with a substrate or nucleotide, and binding to the enzyme

is favorable only as a complex with a substrate or nucleotide molecule. For example, Ha-ras p21 protein, which binds MgGTP (Fig. 1), and the effector site on phosphofructokinase (Fig. 7(b)) where binding of MgADP alters the active conformation of the enzyme. Type B magnesium is characterized by a close association with the enzyme, such that even in the absence of substrate magnesium ion will favorably bind to the active site. Examples include the Mg^{2+} binding sites on xylose isomerase (Fig. 6(b)) or RuBisCO (Fig. 9(a)). We further define magnesium as a type C ion if it serves a catalytic role, while type D domains are structural sites where Mg^{2+} is located in an enzyme pocket that may lie some distance from the substrate binding site. For example, the structural sites in xylose isomerase (Fig. 6(c), (d)) and alkaline phosphatase (Fig. 4). It is clear from the data in Figs. 1–12 that type D structural sites tend to maintain the largest number of enzyme residue contacts to magnesium (anywhere from 4 to 6 per ion). Although it is readily apparent that in some cases the boundaries between these various categories may not be so clear-cut, we find this classification scheme to be generally useful for defining magnesium binding domains in biological systems.

Close inspection of the figures documented throughout the text reveals an important characteristic of binding sites on magnesium proteins, namely, a preference for carboxylate residues as ligands. Every protein or enzyme site shown has at least one (Ha-ras p21 has only one) carboxylate residue in the coordination sphere. This can be rationalized in simple terms by hard/soft criteria inasmuch as the hard magnesium cation prefers to coordinate with hard anions. There is also a clear preference for H_2O as a ligand (with the possible exceptions of xylose isomerase and pyruvate kinase). This reflects the steric difficulties of packing larger protein-derived ligands around the small Mg^{2+} ion. As for oligonucleotide binding, there are often hydrogen-bond contacts from Mg^{2+}-bound H_2O to heteroatoms on the protein backbone and sidechains that contribute to the binding energy of the metal co-factor. In those cases where data of sufficient accuracy affords insight on bond distances (shown as insets in Figs. 1–5, 9, and 10) it is clear that Mg–ligand distances typically fall in the range 1.9–2.5 Å. We would argue that in those cases where ligand atoms are located at a distance greater than 3 Å then there is either no direct interaction, or the interaction is through a hydrogen bond to an unresolved solvent water. As a result of steric clashes with bulky protein sidechains, L–Mg–L′ bond angles often show significant deviations from octahedral geometry (Table 4).

In contrast to calcium proteins, no overall binding motif or "pocket" (including secondary structure) has been clearly identified for magnesium-dependent enzymes. This may reflect the coordination requirements for the multi-functional role of magnesium ion in biology, which serves as a structural agent, a background electrolyte, and a catalytic co-factor in a wide variety of chemical transformations.

Although the number of specific examples is relatively few, the most thoroughly characterized metal binding sites are those identified in high resolution crystallographic data on oligonucleotide samples. From these examples, it would appear that

TABLE 2

Summary of magnesium coordination sites on proteins and enzymes

Enzyme	Binding Site	Ligands
Alkaline phosphatase (*E. coli*)	Structural site	H_2O, H_2O, H_2O, Asp-51, Glu-322, Thr-155
Che Y (*E. coli*)	Active site	Asn(O)-59[a], Asp-57, Asp-13, H_2O[b], Asp-12 SO_4^{2-}
Enolase (yeast)	Allosteric site	Asp-246, Glu-295, Asp-320, O(3)2PG[c], H_2O
3′,5′-Exonuclease Pol I	Active site metal A	Asp-501, Glu-357, Asp-355, H_2O, OP[d]
	Active site metal B	H_2O, H_2O, Asp-355, O_2P[d]
Fructose-1,6-bisphosphatase (pig kidney)	Active site	Glu-280, Asp-121, Asp-118, Glu-97, P(1)F2,6BP, ?[e]
Glutamine synthetase (*Salmonella typhimurium*)	Inner metal site	Glu-131, Glu-220, Glu-212, H_2O, H_2O, H_2O
	Outer metal site	Glu-357, Glu-129, His-269, H_2O, H_2O, H_2O
Ha-ras p21	Active site (before reaction)	Ser-17, P(γ)GTP, P(β)GTP, Thr-35, H_2O, H_2O
	Active site (after reaction)	Ser-17, Asp-57, P(β)GTP, H_2O, H_2O, H_2O
Phosphofructokinase (*E. coli*)	Active site (after reaction)	Asp-103, P(1)F1,6BP, H_2O, H_2O, H_2O, P(β)ADP
	Effector site	Gly(CO)-185[f], H_2O, H_2O, Glu-187, P(β)ADP, P(α)ADP
Pyruvate kinase (skeletal muscle)	Active site (before reaction)	Ala(CO)-292[f], Arg(CO)-293[f], Glu-271, OP-enolpyruvate, ?, ?[e]
	ADP binding site	Ser-242, OP-enolpyruvate, Asp-112, P(α)ADP, P(β)ADP, ?[e]
Ribulose-1,5-bisphosphate carboxylase (RuBisCO) (*Rubrus Rubrum*)	Active site (ternary complex)[g]	Asn-111[h], Glu-194, Asp-193, Lys-191(CO_2^-), H_2O, H_2O
	Active site (quarternary complex)[i]	Glu-194, Lys-191(CO_2^-),?, O(2)rubisco, O(6)rubisco
Xylose isomerase (*Actinoplanes Missouriensis*)	Active site (1) (no substrate)	Asp-245, Glu-181, Glu-217, Asp-292
	Active site (1) (with substrate)	Asp-245, Glu-181, Glu-217, Asp-292, O(2)xylitol, O(4)xylitol
	Active site (2) (no substrate)	His-220, Asp-255, Asp-257, Asp-255, Glu-217, H_2O
	Active site (2) (with substrate)	His-220, Asp-255, Asp-257, O(1)xylitol, Glu-217, H_2O

[a]The asparagine is bound through the amide oxygen.

[b]A water molecule was not actually observed in this structure; however, it is suggested here since the structural data provides no evidence of deviation from the standard octahedral coordination geometry adopted by Mg^{2+} (see Fig. 5).

TABLE 3

General categorization of magnesium binding domains

Enzyme/protein	Category of magnesium site[a]			
	A	B	C	D
Ha-ras p21	×			×
Enolase Mg^{2+} (1)		×	×	
Mg^{2+} (2)	×			×
Fructose 1,6-bisphosphatase		×		×
Xylose isomerase Mg^{2+} (1)		×		×
Mg^{2+} (2)		×		×
Alkaline phosphatase		×	×	
Che Y		×		×
Ribonuclease H		×		×
Phosphofructokinase Mg^{2+} (1, 2)		×		×
Mg^{2+} (3)		×	×	
Mg^{2+} (ATP)	×			×
Pyruvate kinase Mg^{2+} (ATP)	×			×
Mg^{2+}		×		×
RuBisCO		×		×
Glutamine synthetase Mg^{2+} (1)		×		×
Mg^{2+} (2)		×		×
Exonuclease (Pol I)[b]		×		×

[a]The various categories of binding site are defined as follows: A = metal ion binds predominantly to the substrate molecule with weak binding to the protein or enzyme; B = protein/enzyme possesses a well-defined pocket that binds Mg^{2+} with moderate affinity in the absence of substrate; C = magnesium principally serves a structural role; D = magnesium principally serves a catalytic role.

[b]A second putative magnesium ion has not been structurally characterized.

TABLE 2 (*continued*)

[c]This notation indicates coordination through an oxygen on the third carbon in 2-phosphoglycerate.

[d]This notation refers to the diester phosphate of the DNA backbone where either one (OP) or two (O_2P) oxygen atom(s) is/are bound to the metal ion, respectively.

[e]'?' indicates either a ligand of unknown identity or a vacant coordination site on the ion.

[f]Indicates coordination through the main chain carbonyl.

[g]A term used to describe the complex between ribulose 1,5-bisphosphate carboxylase, Mg^{2+}, and the carbamate derived from lysine.

[h]It is not clear from the structural data if asparagine is bound through the oxygen or nitrogen atom.

[i]A term used to describe the complex between ribulose 1,5-bisphosphate carboxylase, Mg^{2+}, carbamate, and ribulose-1,5-bisphosphate.

TABLE 4

Bond angles for magnesium co*factors in enzyme active sites[a]

Alk. phosphatase[b]		CheY[c]		Enolase[d]		F*1,6*BPase[e]		Ha-Rasp21[f]		RuBisCO[g]	
Ligands	L–M–L′ (°)	Ligands	L–M–L′ (°)	Ligands	L–M–L′ (°)	Ligands	L–M–L′ (°)	Ligands	L–M–L′ (°)	Ligands	L–M–L′ (°)
Asp51	101.1	Asp12	82.70	Glu295	93.89	Asp118	140.36	Ser17	82.81	Asp193	165.33
Thr155	83.7	Asn59	105.83	Asp320	171.97	Glu280	74.21	βP(O)	173.42	Glu194	72.74
Glu322	152.9	Asp57	161.17	Enolate(O)	87.13	Glu97	149.11	γP(O)	91.26	Lys191(CO)	121.66
W454	86.5	W	66.49	W	137.91	Asp121	54.78	W1	90.46	Lys191(CO)	67.00
W455	76.7	SO_4^{2-}	160.40					W2	89.31		

[a]Bond angles are taken from crystallographic data deposited in the Brookhaven Data Bank.
[b]Angles are measured relative to W456 in Fig. 4.
[c]Angles are measured relative to Asp13 in Fig. 5.
[d]Angles are measured relative to Asp246 in Fig. 2.
[e]Angles are measured relative to X ligand in Fig. 3.
[f]Angles are measured relative to Thr35 in Fig. 1(a).
[g]Angles are measured relative to W1 in Fig. 9(a).

outer sphere coordination of a hydrated metal center is much more common than direct inner sphere contacts. The rationale and implications of this observation have been discussed elsewhere [2,72]. Typically, Mg–OH_2 distances fall in the range 2.0–2.2 Å and H_2O–Mg–OH_2 bond angles lie between 80 and 100° (most commonly 85–95°). In those cases where inner sphere binding has been identified, larger deviations are observed (Table 5). The apparent affinity of metal ions for N7 of guanosine most likely results from steric constraints that position the metal ion close to this ligand atom.

The apparent tendency for protein binding domains to adopt inner sphere coordination to Mg^{2+} relative to the outer sphere interactions common to nucleic

TABLE 5

Bond angles between the magnesium complex and the oligonucleotides[a]

Oligonucleotides[b]	Mg–X–L[c]	Angle (°)	Mg–X–L[c]	Angle (°)
d(CGCGCG)	A′–W–Op (G6)	142.23	A′–W–O4′ (G6)	151.51
	A′–W–Op (C5)	121.90		
	B′–W–O6 (G4)	145.24	B′–W–N7 (G8)	129.69
	C′–W–W (B′)	152.22	C′–W–D′	82.46[d]
	C′–W–D′	87.62[d]		
	D′–W–N7 (G10)	130.86	D′–W–O6 (G10)	120.97
	D′–W–N4 (C3)	114.21		
$tRNA^{Phe}$	Mg–W–Op (U12)	115.68	Mg–W–Op (U12)	82.62
	Mg–W–Op (C11)	114.89	Mg–W–Op (U8)	90.67
	Mg–W–Op (A9)	142.32		
	Mg–Op–P (G20)	154.36	Mg–Op–P (A21)	145.54
	Mg–Op–P (G19)	132.06	Mg–W–O6 (G20)	127.39
	Mg–W–N7 (G20)	108.84	Mg–W–O4 (U59)	156.27
	Mg–W–N4 (C60)	122.01		
	Mg–O–P (Y37)	163.81	Mg–W2–O2 (Ψ39)	121.96
	Mg–W3–N7 (A38)	121.26	Mg–W3–N6 (A38)	120.82
	Mg–W3–N7 (Y37)	123.89	Mg–W4–O2 (C32)	130.4
	W1–Mg–Op (Y37)	112.18	W2–Mg–Op (Y37)	67.79
	W3–Mg–Op (Y37)	119.25	W4–Mg–Op (Y37)	149.15
	W5–Mg–Op (Y37)	69.71		

[a]Bond angles are measured from the crystallographic data deposited in the Brookhaven Data Bank. Since H_2O–Mg–O_2H angles for hydrated Mg^{2+} typically fall in the range 85–95°, emphasis is placed on the surrounding hydrogen bond network.

[b]Sites in d(CGCGCG) are illustrated in Fig. 16 and those for $tRNA^{Phe}$ in Fig. 21. The notation A′, B′, ... etc., denotes the Mg^{2+} ion in the particular complex with that label in Fig. 16.

[c]X indicates either the oxygen atom of the coordinated water molecule (W) or the directly coordinated oxygen atom of the oligonucleotide phosphate backbone. The notation Op denotes an outer sphere interaction between the phosphate backbone and a water of hydration (W), while O–P indicates inner sphere coordination by phosphate.

[d]The angle refers to the bridging water molecules that connect sites C′ and D′ in Fig. 16.

acids stems from the nature of the chelating pockets formed by a protein binding domain that favor direct coordination. The few inner sphere magnesium ions identified in structural data on $tRNA^{Phe}$ are also located in such chelating environments. In this regard, the inherent lability of divalent magnesium must be considered in any functional role for the metal ion in the context of enzyme mechanism, inasmuch as the structurally most stable configuration may not represent the functionally competent coordination state of the metal during enzyme turnover [2,77].

ACKNOWLEDGMENTS

We thank Dr. L.-Y. Hsu for assistance with molecular graphics analysis. Our research on the biological chemistry of alkali and alkaline earth metals is supported in part by the Petroleum Research Research Fund (administered by the American Chemical Society). J.A.C. is a Fellow of the Alfred P. Sloan Foundation and a National Science Foundation Young Investigator.

REFERENCES

1 J.J.R. Frausto da Silva and R.J.P. Williams, The Biological Chemistry of the Elements, Oxford University Press, Oxford, 1991.
J.A. Cowan, Inorganic Biochemistry. An Introduction, VCH, in press.
2 J.A. Cowan, Comments Inorg. Chem., 13 (1992) 293; Inorg. Chem., 30 (1991) 2740.
3 E.F. Pai, U. Krengel, G.A. Petsko, R.S. Goody, W. Kabsch and A. Wittinghofer, EMBO J., 9 (1990) 2351.
4 E.F. Pai, W. Kabsch, U. Krenger, K.C. Holmes, J. John and A. Wittinghofer, Nature, 341 (1989) 209.
5 I. Schlichting, S.C. Almo, G. Rapp, K. Wilson, K. Petratos, A. Lentfer, A. Wittinghofer, W. Kabsch, E.F. Pai, G.A. Petsko and R. Goody, Nature, 354 (1990) 309.
6 L. Leiboda and B. Stec, Biochemistry, 30 (1991) 2817.
7 L.D. Faller, B.M. Baroudy, A.M. Johnson and R.X. Ewall, Biochemistry, 16 (1977) 3864.
8 J. Stubbe and R.H. Abeles, Biochemistry, 19 (1980) 5505.
9 H. Ke, Y. Zhang and W.N. Lipscomb, Proc. Natl. Acad. Sci. U.S.A., 87 (1990) 5243.
10 S.J. Pilkis, T.H. Claus, P.D. Kountz and M.R. EL-Maghrabi, in P.D. Boyer and E.G. Krebs (Eds.), The Enzymes, Vol. 18, Academic Press, Orlando, 3rd edn., 1987, pp. 3–46.
11 H. Ke, J.-Y. Liang and W.N. Lipscomb, Proc. Natl. Acad. Sci. U.S.A., 88 (1991) 2989.
12 T.W. Reid and I.B. Wilson, in P.D. Boyer (Ed.), The Enzymes, Vol. 4, Academic Press, New York, 3rd edn., 1971, pp. 373–415.
13 H.N. Fernly, in P.D. Boyer (Ed.), The Enzymes, Vol. 4, Academic Press, New York, 3rd edn., 1971, pp. 417–447.
14 E.E. Kim and H.W. Wyckoff, J. Mol. Biol., 218 (1991) 449.
15 W.F. Bosron, R.A. Anderson, M.C. Falk, E.S. Kennedy and B.L. Vallee, Biochemistry, 16 (1977) 610.
16 J.M. Sowadski, M.D. Handschumacher, H.M. Krishna Murthy, B.A. Foster and H.A. Wyckoff, J. Mol. Biol., 186 (1985) 417.
17 R.B. Bourret, J.F. Hess and M.I. Simon, Proc. Natl. Acad. Sci. U.S.A., 87 (1990) 41.
18 K. Volz and P. Matsumura, J. Biol. Chem., 266 (1991) 15511.

19 T. Itoh and J. Tomizawa, Proc. Natl. Acad. Sci. U.S.A., 77 (1980) 2450.
20 K. Mölling, D.P. Bolognesi, H. Bauer, W. Büsen, H.W. Plassmann and P. Hausen, Nature New Biol., 234 (1971) 240.
21 W. Keller and R.J. Crouch, Proc. Natl. Acad. Sci. U.S.A., 69 (1972) 3360.
22 M. Katayanagi, M. Miyagawa, M. Ishikawa, S. Kanaya, M. Ikehara, T. Matsuzaki and K. Morikawa, Nature, 347 (1990) 306.
23 R.D. Banks, C.C.F. Blake, P.R. Evans, R. Haser, D.W. Rice, G.W. Hardy, M. Merrett and A.W. Phillips, Nature, 279 (1979) 773.
24 F.J. Kayne, in P.D. Boyer (Ed.), The Enzymes, Vol. 8, Academic Press, New York, 3rd edn., 1973, pp. 353–364.
25 H. Yan and M.D. Tsai, Biochemistry, 30 (1991) 5539.
26 T.K. White and J.E. Wilson, Arch. Biochem. Biophys., 277 (1990) 26.
27 J.P. Jones, P.M. Weiss and W.W. Cleland, Biochemistry, 30 (1991) 3634.
28 J. Jenkins, J. Janin, F. Rey, M. Chiadmi, H. van Tilbeurgh, I. Lasters, M. De Maeyer, D. Van Belle, S.J. Wodak, M. Lauwereys, P. Stanssens, N.T. Mrabet, J. Snauwaert, G. Matthyssens and A.M. Lambeir, Biochemistry, 31 (1992) 5449.
29 G.K. Farber, A. Glasfeld, G. Tiraby, D. Ringe and G.A. Petsko, Biochemistry, 28 (1989) 7289.
30 H. Van Tilbeurgh, J. Jenkins, M. Chiadmi, J. Janin, S.J. Wodak, N.T. Mrabet and A.M. Lambeir, Biochemistry, 31 (1992) 5467.
31 C.A. Collyer, K. Henrick and D.M. Blow, J. Mol. Biol., 212 (1990) 211.
32 Y. Shirakihara and P.R. Evans, J. Mol. Biol., 204 (1988) 973.
33 J.M. Van Divender and C.M. Grisham, J. Biol. Chem., 260 (1985) 14060.
34 H. Muirhead, D.A. Clayden, S.P. Cuffe and C. Davies, Biochem. Soc. Trans., 15 (1987) 996.
35 D.I. Stuart, M. Levine, H. Muirhead and D.K. Stammers, J. Mol. Biol., 134 (1979) 109.
36 T.J. Andrews and G.H. Lorimer, in M.D. Hatch (Ed.), The Biochemistry of Plants, Vol. 10, Academic Press, Orlando, 1987, pp. 131–218.
37 G.H. Lorimer and H.M. Miziorko, Biochemistry, 19 (1980) 5321.
38 T. Lundqvist and G. Schneider, Biochemistry, 30 (1991) 904.
39 S. Knight, I. Andersson and C.I. Branden, J. Mol. Biol., 215 (1990) 113.
40 (a) G. Schneider, Y. Lundqvist and T. Lundqvist, J. Mol. Biol., 211 (1990) 989.
(b) T. Lundqvist and G. Schneider, J. Biol. Chem., 266 (1991) 12604.
41 R.J. Almassey, C.A. Janson, R. Hamlin, X.H. Xuong and D. Eisenberg, Nature, 323 (1986) 304.
42 E.R. Stadtman and A. Ginsburg, in P.D. Boyer (Ed.), The Enzymes, Vol. 10, Academic Press, New York, 3rd edn., 1974, pp. 755–807.
43 R.A. Alberty, J. Biol. Chem., 243 (1968) 1337.
44 M.Y. Yamashita, R.J. Almassy, C.A. Janson, D. Cascio and E. Eisenberg, J. Biol. Chem., 264 (1989) 17681.
45 D.L. Ollis, P. Brick, R. Hamlin, J.G. Xuong and T.A. Steitz, Nature, 313 (1985) 762.
46 V. Derbyshire, P.S. Freemont, M.R. Sanderson, L. Beese, J.M. Friedman, C.M. Joyce and T.A. Steitz, Science, 240 (1988) 199.
47 H. Hyunsoo, J.M. Rifkind and A.S. Mildvan, Biochemistry, 30 (1991) 11104.
48 L.S. Beese and T.A. Steitz, EMBO J., 10 (1991) 25.
49 G.P. Mullen, E.H. Serpersu, L.J. Ferrin, L.A. Loeb and A.S. Mildvan, J. Mol. Biol., 265 (1990) 14327.
50 P.D. Boyer, H.A. Lardy and P.H. Phillips, J. Biol. Chem., 146 (1942) 673.
51 L.A. Edwards, M.R. Tian, R.E. Huber and A.V. Fowler, J. Biol. Chem., 263 (1988) 1848.
52 C.H. Suelter, Science, 168 (1970) 789.

53 T.J. Beveridge and R.G.E. Murray, J. Bacteriol., 127 (1976) 1502.
54 H. Hauser, B.A. Levine and R.J.P. Williams, Trends Biochem. Sci., 1 (1976) 278.
55 E.I. Ochiai, in E. Frieden (Ed.), Biochemistry of the Elements, Vol. 7, Plenum Press, New York, 1987, p. 205.
56 D.J. Triggle, Prog. Surf. Membr. Sci., 5 (1972) 267.
57 P.A. Agron and W.R. Busing, Acta Crystallogr. Sect. C, 41 (1985) 8.
58 P.S. Ho, C.A. Frederick, G.J. Quigley, G.A. van der Marel, J.H. van Boom, A.H.-J. Wang and A. Rich, EMBO J., 4 (1985) 3617.
59 R.V. Gessner, G.J. Quigley, A.H.-J. Wang, G.A. van der Marel, J.H. van Boom and A. Rich, Biochemistry, 24 (1985) 237.
60 M. Coll, D. Saal, C.A. Frederick, J. Aymami, A. Rich and A.H.-J. Wang, Nucl. Acids Res., 17 (1989) 911.
61 R.V. Gessner, C.A. Frederick, G.J. Quigley, A. Rich and A.H.-J. Wang, J. Biochem., 264 (1989) 7921.
62 J.R. Quintana, K. Grzeskowiak, K. Yanagi and R.E. Dickerson, J. Mol. Biol., 225 (1992) 379.
63 W.B.T. Cruse, S.A. Salisbury, T. Brown, R. Cosstick, F. Eckstein and O. Kennard, J. Mol. Biol., 192 (1986) 891.
64 A.H.-J. Wang, T. Hakoshima, G.A. van der Marel, J. H. van Boom and A. Rich, Cell, 37 (1984) 321.
65 B. Chevrier, A.C. Dock, B. Hartmann, M. Leng, D. Moras, M.T. Thuong and E. Westhof, J. Mol. Biol., 188 (1986) 707.
66 W.I. Sundquist and A. Klug, Nature, 342 (1989) 825.
67 C.D. Stout, H. Mizuno, S.T. Rao, P. Swaminathan, J. Rubin, T. Brennan and M. Sundaralingam, Acta Crystallogr. Sect. B, 34 (1978) 1529.
68 S.-H. Kim, Topics Mol. Struct. Biol., 1 (1981) 83.
69 S.R. Holbrook, J.L. Sussman, R.W. Warrant, G.M. Church and S.-H. Kim, Nucl. Acids Res., 8 (1977) 2811.
70 G.J. Quigley, M.M. Teeter and A. Rich, Proc. Nat. Acad. Sci. U.S.A., 75 (1978) 64.
71 A. Jack, J.E. Ladner. D. Rhodes, R.S. Brown and A. Klug, J. Mol. Biol., 111 (1977) 315.
72 S.S. Reid and J.A. Cowan, Biochemistry, 29 (1990) 6025 and references cited therein. J.A. Cowan, J. Am. Chem. Soc., 113 (1991) 675.
73 T.R. Cech and B.L. Bass, Annu. Rev. Biochem., 55 (1986) 599.
74 C.J. Hutchins, P.D. Rathjen, A.C. Foster and R.H. Symons, Nucl. Acids Res., 14 (1986) 3627.
75 A.C. Foster and R.H. Symons, Cell, 49 (1987) 211.
76 C. Guerrier-Takada, K. Haydock, L. Allen and S. Altman, Biochemistry, 25 (1986) 1509.
77 R. Jou and J.A. Cowan, J. Am. Chem. Soc., 113 (1991) 6685.
78 W. Saenger, Principles of Nucleic Acid Structure, Springer-Verlag, New York, 1984, pp. 290–293.